Next Generation Very Large Array Memo #72
A Study of ngVLA Subarray Efficiency: Plains + Fractions of the Core

Viviana Rosero (NRAO)

January 15, 2020

Abstract

In this memo I present five subarrays that each consist of the entire Plains subarray plus different fractions of the Core subarray. For each subarray I calculate the taperability, i.e., the change in sensitivity versus resolution, and the PSF resulting from a 4-hour simulation at 30 GHz. I analyze the taperability curves and compare the efficiencies of these subarrays over a range of representative resolutions. I find that subarrays with fewer core antennas are more efficient at certain resolutions, and discuss how the consideration of subarray efficiency could be used to construct a high-throughput observing program (e.g., one that minimizes the time needed to complete all the KSG observations).

1 Introduction

The ngVLA reference design is comprised of three fundamental subsets, the Main Array (MA), the long baseline array (LBA) and the short baseline array (SBA). Depending on the science requirements, the ngVLA can in principle operate with combinations of different subarrays and/or subsets. In ngVLA memo #55 [3] I presented a study of the simulated image noise at different angular resolutions, achieved by varying the imaging weights, for six subsets and subarrays of the ngVLA that include the Main, LBA, Main+LBA, Mid−baseline, Plains+Core and Core. By studying the change in sensitivity versus resolution of different subarrays I concluded that the current ngVLA reference design has a high degree of taperability, i.e., it can accommodate a wide range of resolutions without a great loss of sensitivity. In order to account for the change in sensitivity due to use of imaging weights (relative to the naturally weighted rms defined as σ_{NA}), I used an efficiency factor η_{weight}[1] such that the expected image rms after weighting is $\sigma_{rms} = \eta_{weight}\sigma_{NA}$.

[1] Or an 'innefficiency' factor for this effect.

As it has been pointed out in previous memos by C. Carilli (e.g., ngVLA memo #12 [1] and ngVLA memo #41 [2]) the centrally condensed antenna distribution of the ngVLA leads to a natural point spread function (PSF) that is not well characterized by a Gaussian, and therefore any subarray that contains the ngVLA Core will produce a naturally weighted beam (both tapered and untapered) that features a type of PSF non-Gaussianity which is often referred to as a beam 'skirt' or 'plateau'. However, ngVLA memo #55 [3] and ngVLA memo #65 [4] show that combinations of robustness and tapering allow for a beam of much higher quality but at the expense of sensitivity. For example, ngVLA memo #55 [3] presented a first approximation of beam sculpting by using Briggs weighting with a value of robust R= -0.5, which reduced the skirt to an acceptable level with a typical loss of sensitivity of less than a factor of two ($\eta_{weight} < 2$) compared to natural weighting.

The ngVLA notional reference observing program (ROP) [5] presents a systematic quantification of the technical and observing needs of the key science goals (KSGs) which are the drivers of the ngVLA reference design. The ROP is expressed in terms of the subset or subarray times needed by those KSGs, wherein the Plains+Core is a frequently assigned subarray based on the general approach explained in the ROP document [5] Section 3, paragraph 3. The fundamental requirements for this assignment are the achievable resolution and largest angular scale (LAS) at the frequency specific to each KSG. Additionally, the ROP states that "If more than one subset or subarray can meet the use case requirements, the one that will minimize T_{target} is generally picked."

It is important to point out that if T_{target} is used as a strong criteria in the assignment of a subarray then we may be incurring a loss in the overall efficiency of ngVLA operations. For example, a subarray selected in this manner may produce too many short baselines and lead to an unacceptable PSF with a large skirt. In order to meet the KSG's specific scientific requirements it may then be required to adjust the image parameters to 'sculpt' a more appropriate synthesized beam, which introduces inefficiency by down-weighting these undesirable short baselines. *Instead of using T_{target} to choose the subarray with the highest performance, I would like to propose that we could optimize the scientific throughput by selecting the subarray that minimizes the inefficiency parameter η_{weight}.*

In this memo I present a taperability study of five subarrays that include the Plains subarray plus a fraction of the Core, namely: Plains (alone; no-Core), Plains+10th Core, Plains+Quarter Core, Plains+Third Core, Plains+Half Core. These results are compared with the simulations of the Plains + (Full) Core subarray, which was originally presented in ngVLA memo #55 [3]. The primary goal of this memo is to study how the taperability, efficiency and quality of the synthesized beam changes as a function of the number of Core antennas used together with the Plains subarray. Additionally, a taperability study of the ngVLA Plains+Mid-baseline subarray is included in the appendix Section

C as a potentially interesting subarray.

The simulations and imaging presented in this work are described in ngVLA memo #55 [3] Section 2. Tables 1, 2, 3, 4, 5 and 11 in Appendix A show the simulation parameters for each of the subarrays studied in this memo. For a description of each column of these tables please refer to ngVLA memo #55 [3] Section 3.

Figures 2, 5, 8, 11, 14 and 23 show the change in sensitivity with resolution, i.e., the taperability, at 30 GHz for each simulations. The plotted resolutions ($\theta_{1/2}$) correspond to the geometric mean of the minor and major beam FWHM reported in the tables of simulation parameters. The taperability results are then used to provide tables of key performance metrics for each subarray (Appendix B) at several representative resolutions. The sensitivity calculations in the key performance tables include η_{weight}, estimated using the blue and red data series in the taperability figures and by scaling $\theta_{1/2}$ with frequency as $\theta_{1/2@30GHz} = \theta_{1/2@\nu} \times (\nu/30\,\mathrm{GHz})$, where $\theta_{1/2}$ is in mas.

2 Study of Subarrays that Include the Plains+Fractions of the Core

2.1 ngVLA Plains Subarray

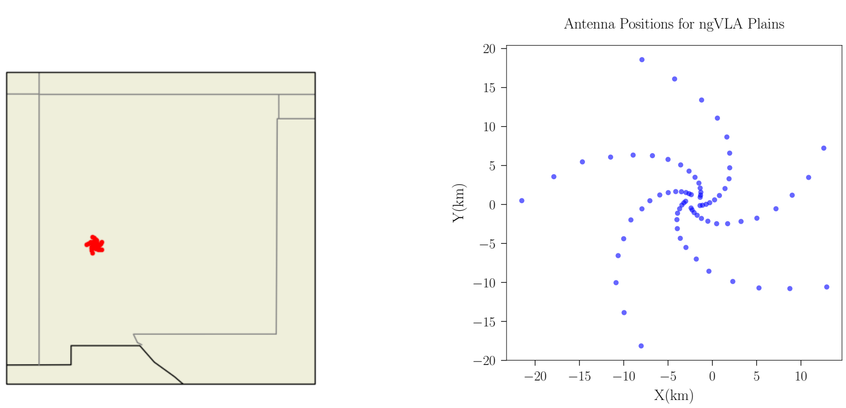

Figure 1: Positions of the 74 18 m antennas for the Plains subarray.

Figure 1 shows the position of the antennas of the Plains subarray –which excludes the 94 antennas from the Core. The Plains subarray extends over a maximum baseline of 36.5 km and a minimum baseline of 250 m. For this subarray, the images have a size of 20480 px.

Natural weighting with no uv-taper, which gives the best sensitivity, produces an angular resolution of 96.9 mas. From Figure 2 we see that for natural weighting, we can use a uv-taper to vary the angular resolution over a range of $\theta_{1/2} \sim 67 - 370$ mas for which we pay a penalty in sensitivity of $\lesssim 2$. Likewise, for a range of angular resolution of $\theta_{1/2} \sim 68 - 243$ mas we pay a penalty in sensitivity of $\lesssim 1.5$.

The features of the resulting taperability curve are similar to the ones from the ngVLA Mid-baseline and Core subarrays, i.e., the loss of sensitivity for increasingly large uv-tapers is steep.

Figure 3 shows examples of 1D East-West cuts through example PSFs.

Table 6 in Appendix B shows the key performance metrics of the ngVLA Plains subarray using 74 antennas, tabulated for a range of selected resolutions between 100 and 10000 mas. These metrics include the change in sensitivity corresponding to the uv-taper needed to achieve these resolutions (based on Figure 2 and the frequency scaling described in Section 1).

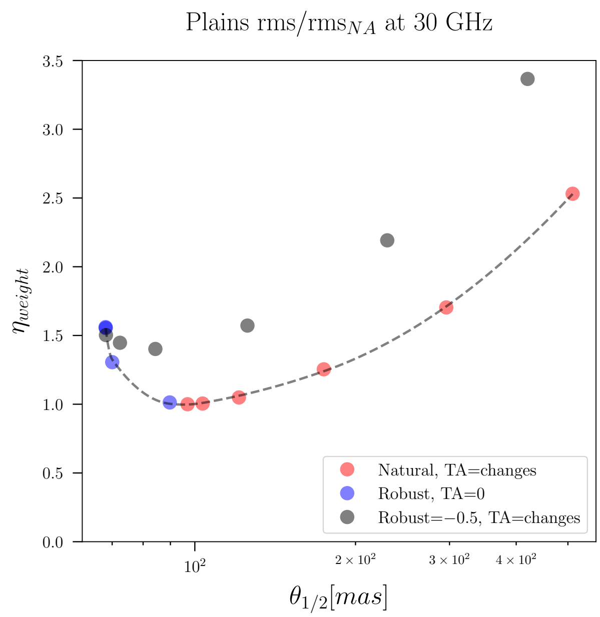

Figure 2: Taperability curve for the ngVLA Plains Subarray showing the image standard deviation (σ) at different angular resolutions (FWHM) achieved by varying the imaging weights, simulated at 30 GHz. The noise has been scaled relative to that of the naturally weighted image (σ_{NA}). The red symbols correspond to use of a uv-taper and natural weights, and the blue symbols to Briggs robust weighting without a taper. The gray symbols are for Briggs robust R= -0.5 and a varying uv-taper, which has a large effect on beam quality (see Figure 3). The dashed line is the interpolation of the points used to estimate η_{weight}.

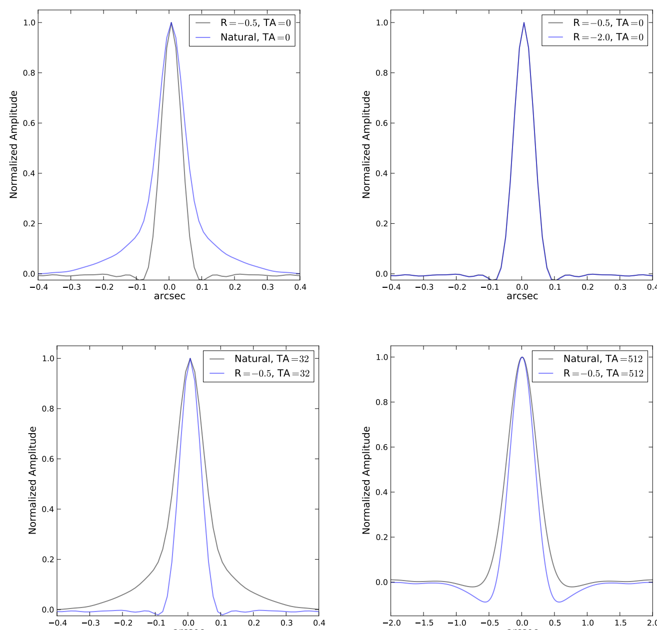

Figure 3: Simulated 30 GHz PSFs for the ngVLA Plains subarray over a range of resolutions, showing the effect of different imaging weights (TA: uv-taper in mas, R: Briggs robust parameter). The PSFs are a selection of the data presented in Table 1. These examples illustrate how combinations of robustness and tapering allow for a beam of much higher quality (but at the expense of sensitivity).

2.2 ngVLA Plains+Half Core Subarray

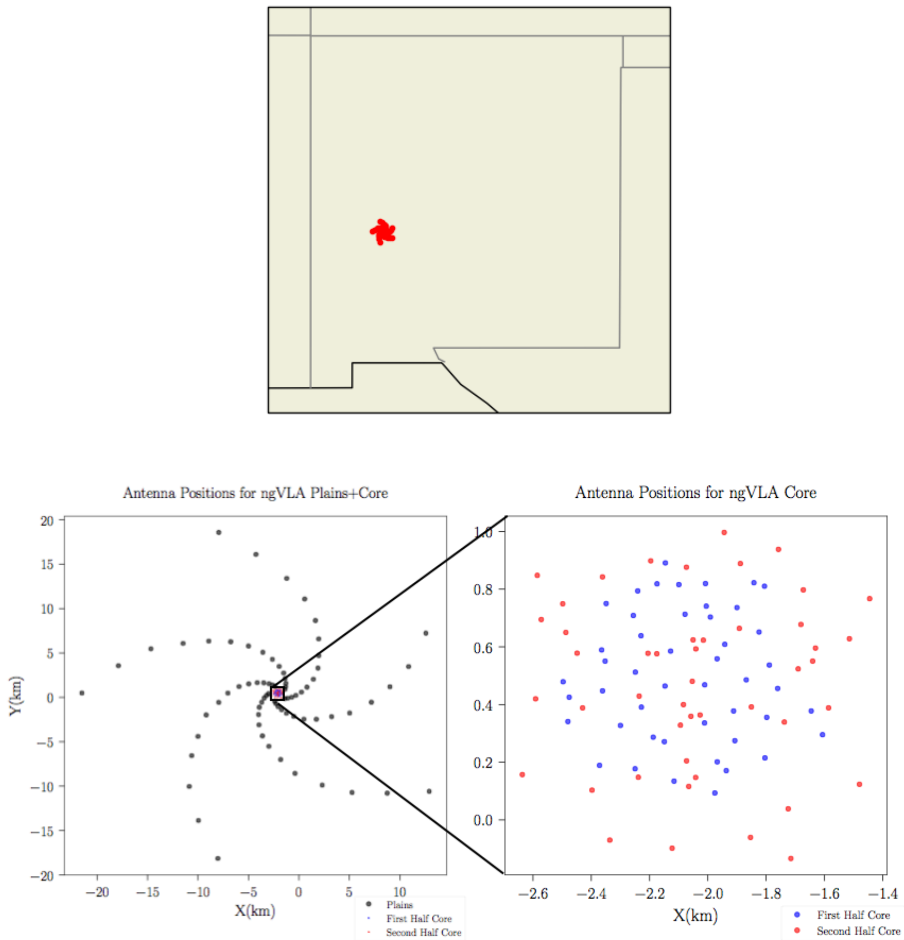

Figure 4: Positions of the 121 18 m antennas for the Plains+Half Core subarray for the first half (blue dots) and second half (red dots) from the configuration file of the ngVLA Core.

Figure 4 shows the position of the antennas of the Plains+Half Core subarray. For these and other simulations where a fraction of the Core is selected, the antennas have been chosen in a simple fashion based on the order that they appear in the configuration file of the Core subarray. The results for the taperability curve and PSF shape are not expected to change significantly based on the selection method, since the selected antennas would still be in approximately the same location (i.e., within the compact, 1.3 km diameter core). However,

a more careful selection could better preserve the shortest baselines present in the Core subarray and therefore retain the LAS of the full Core.
The Plains+Second Half subarray extends over a maximum baseline of 36.5 km and a minimum baseline of 27 m. For this subarray, the images have a size of 20480 px.

Natural weighting with no uv-taper, which gives the best sensitivity, produces an angular resolution of 134.56 mas. From Figure 5 we see that for natural weighting, we can use a uv-taper to vary the angular resolution over a range of $\theta_{1/2} \sim 73 - 1330$ mas for which we pay a penalty in sensitivity of $\lesssim 2$. Likewise, for a range of angular resolution of $\theta_{1/2} \sim 79 - 590$ mas we pay a penalty in sensitivity of $\lesssim 1.5$.

Figure 6 shows examples of 1D East-West cuts through example PSFs.

Table 7 in Appendix B shows the key performance metrics of the ngVLA Plains+Second Half Core subarray using 121 antennas, tabulated for a range of selected resolutions between 100 and 10000 mas. These metrics include the change in sensitivity corresponding to the uv-taper needed to achieve these resolutions (based on Figure 5 and the frequency scaling described in Section 1).

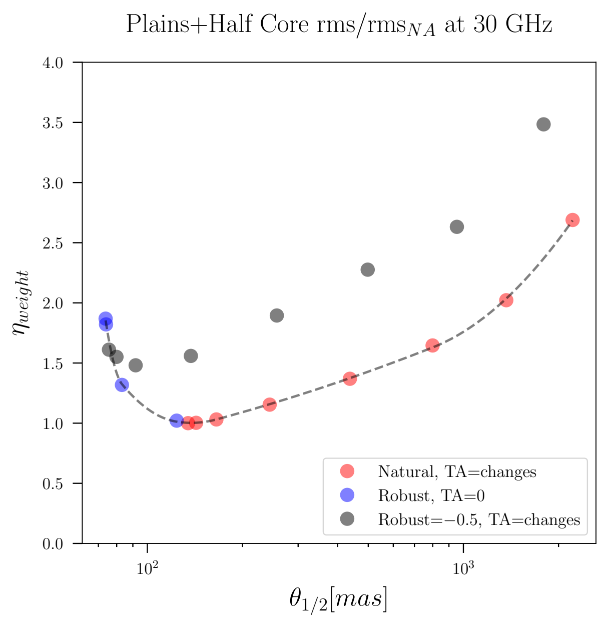

Figure 5: Taperability curve for the ngVLA Plains+Half Core subarray showing the image noise (rms) at different angular resolutions (FWHM) achieved by varying the imaging weights, simulated at 30 GHz. The noise has been scaled relative to that of the naturally weighted image (rms$_{NA}$). Symbols and colors are the same as used in Figure 2.

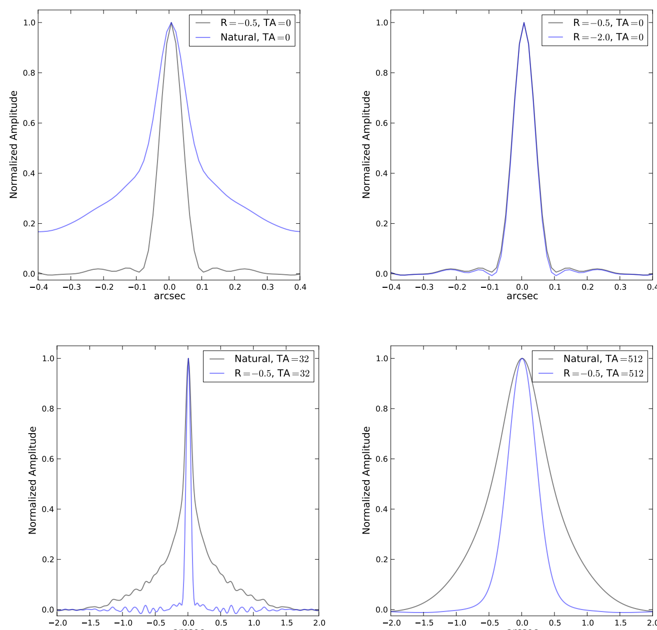

Figure 6: Simulated 30 GHz PSFs for the ngVLA Plains+Second Half Core subarray over a range of resolutions, showing the effect of different imaging weights (TA: uv-taper in mas, R: Briggs robust parameter). The PSFs are a selection of the data presented in Table 2. These examples illustrate how combinations of robustness and tapering allow for a beam of much higher quality (but at the expense of sensitivity).

2.3 ngVLA Plains+Third Core Subarray

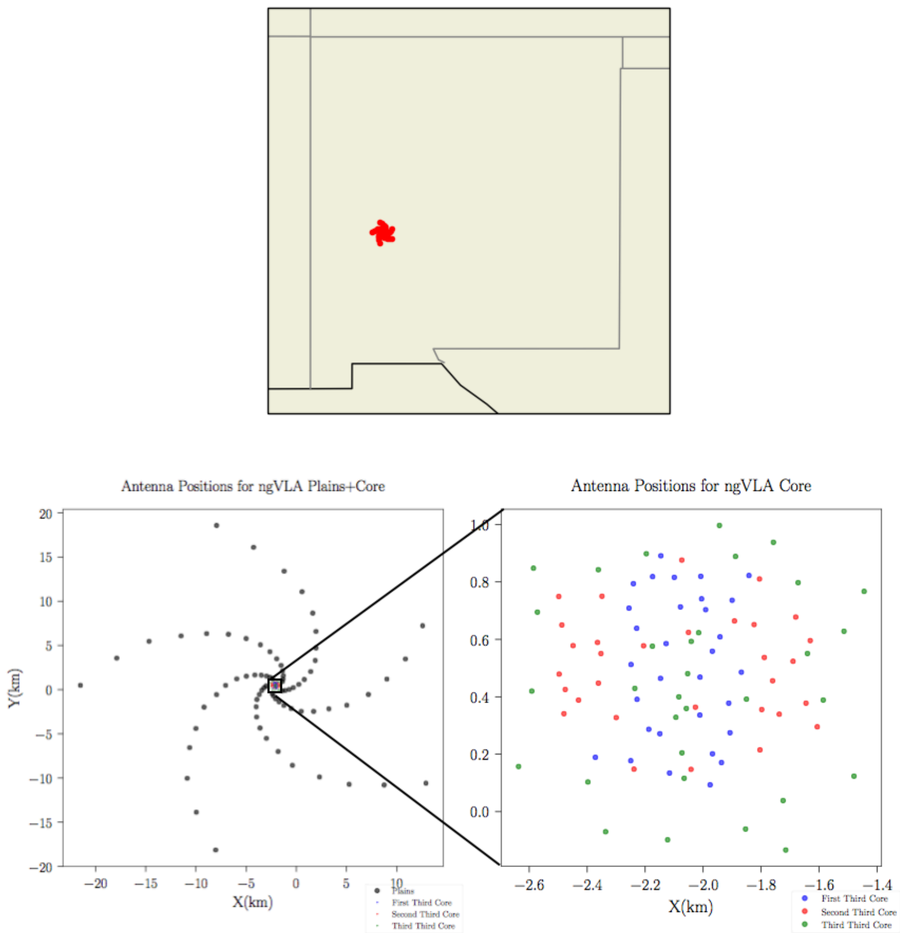

Figure 7: Positions of the 106 18 m antennas for the Plains+Third Core subarray for the last 32 antennas (green dots) of the core configuration file.

Figure 7 shows the position of the antennas of the Plains+Third Core subarray. The Plains+Third Third Core subarray extends over a maximum baseline of 36.5 km and a minimum baseline of 37 m. For this subarray, the images have a size of 20480 px.

Natural weighting with no uv-taper, which gives the best sensitivity, produces an angular resolution of 124.13 mas. From Figure 8 we see that for natural weighting, we can use a uv-taper to vary the angular resolution over a range of

$\theta_{1/2} \sim 71 - 900$ mas for which we pay a penalty in sensitivity of $\lesssim 2$. Likewise, for a range of angular resolution of $\theta_{1/2} \sim 76 - 463$ mas we pay a penalty in sensitivity of $\lesssim 1.5$.

Figure 9 shows examples of 1D East-West cuts through example PSFs.

Table 8 in Appendix B shows the key performance metrics of the ngVLA Plains+Third Core subarray using 106 antennas, tabulated for a range of selected resolutions between 100 and 10000 mas. These metrics include the change in sensitivity corresponding to the uv-taper needed to achieve these resolutions (based on Figure 8 and the frequency scaling described in Section 1).

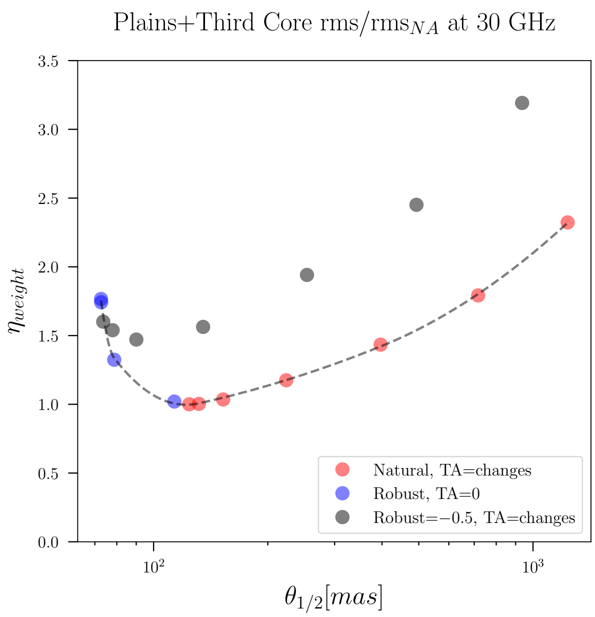

Figure 8: Taperability curve for the ngVLA Plains+Third Core subarray showing the image noise (rms) at different angular resolutions (FWHM) achieved by varying the imaging weights, simulated at 30 GHz. The noise has been scaled relative to that of the naturally weighted image (rms$_{NA}$). Symbols and colors are the same as used in Figure 2.

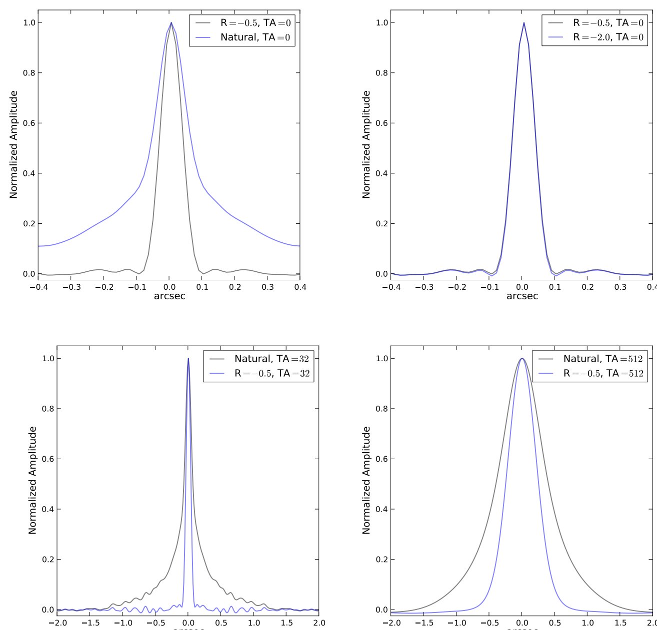

Figure 9: Simulated 30 GHz PSFs for the ngVLA Plains+Third Core subarray over a range of resolutions, showing the effect of different imaging weights (TA: uv-taper in mas, R: Briggs robust parameter). The PSFs are a selection of the data presented in Table 3. These examples illustrate how combinations of robustness and tapering allow for a beam of much higher quality (but at the expense of sensitivity).

2.4 ngVLA Plains+Quarter Core Subarray

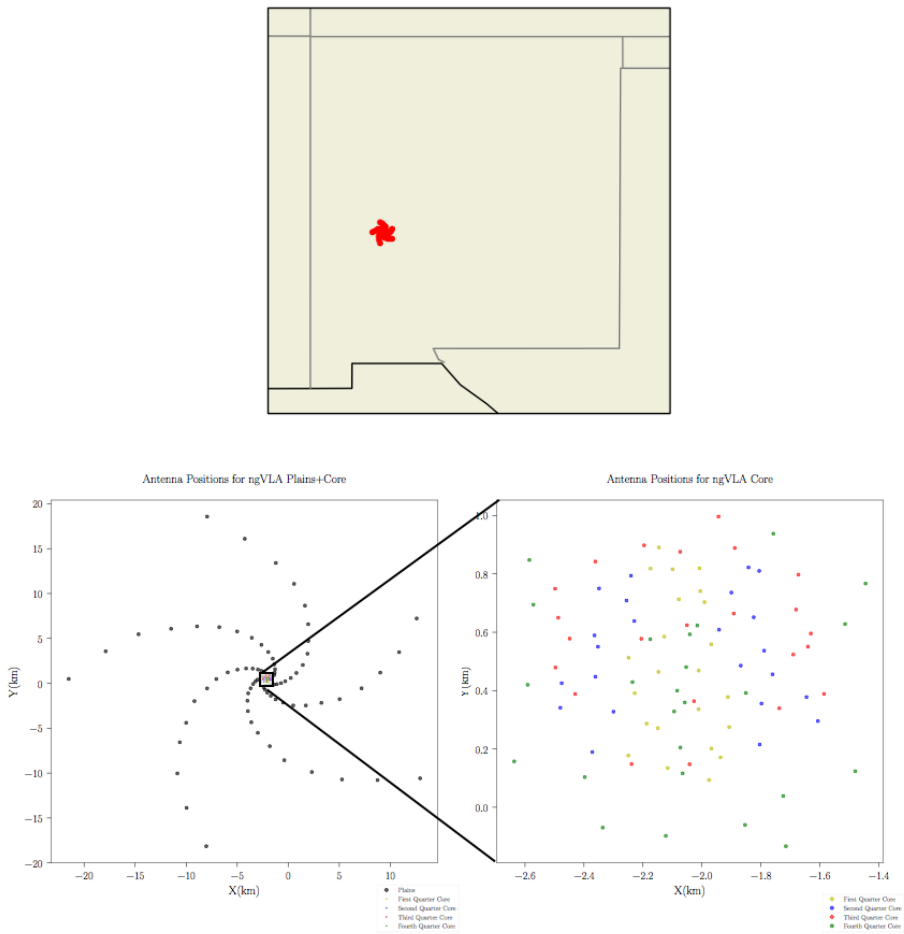

Figure 10: Positions of the 97 18 m antennas for the Plains+Quarter Core subarray for the third quarter of the antennas of the core configuration file (red dots).

Figure 10 shows the position of the antennas of the Plains+Quarter Core subarray. The Plains+Third Quarter Core subarray extends over a maximum baseline of 36.5 km and a minimum baseline of 45 m. For this subarray, the images have a size of 20480 px.

Natural weighting with no uv-taper, which gives the best sensitivity, produces an angular resolution of 116.95 mas. From Figure 11 we see that for natural weighting, we can use a uv-taper to vary the angular resolution over a range of $\theta_{1/2} \sim 70 - 705$ mas for which we pay a penalty in sensitivity of $\lesssim 2$. Likewise, for a range of angular resolution of $\theta_{1/2} \sim 73 - 380$ mas we pay a penalty in sensitivity of $\lesssim 1.5$.

Figure 12 shows examples of 1D East-West cuts through example PSFs.

Table 9 in Appendix B shows the key performance metrics of the ngVLA Plains+Quarter Core subarray using 97 antennas, tabulated for a range of selected resolutions between 100 and 10000 mas. These metrics include the change in sensitivity corresponding to the uv-taper needed to achieve these resolutions (based on Figure 11 and the frequency scaling described in Section 1).

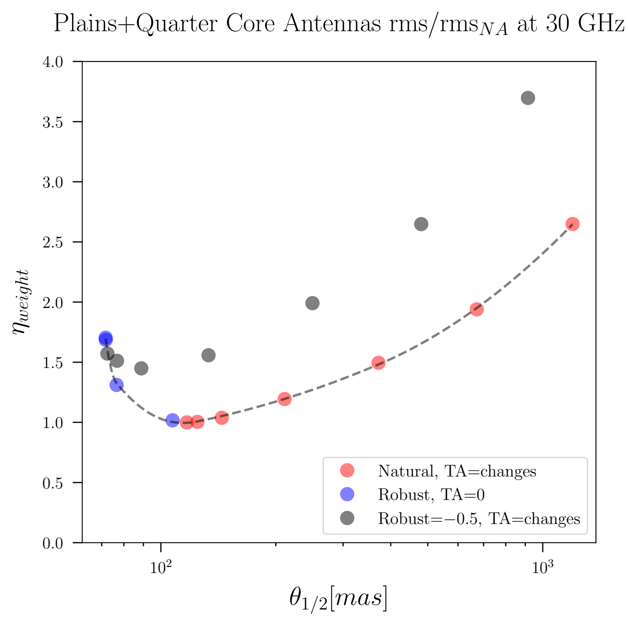

Figure 11: Taperability curve for the ngVLA Plains+Quarter Core subarray showing the image noise (rms) at different angular resolutions (FWHM) achieved by varying the imaging weights, simulated at 30 GHz. The noise has been scaled relative to that of the naturally weighted image (rms$_{NA}$). Symbols and colors are the same as used in Figure 2.

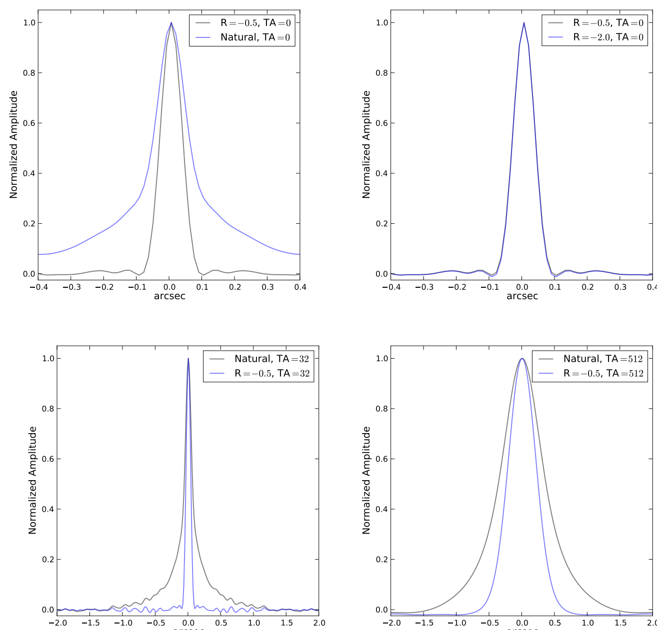

Figure 12: Simulated 30 GHz PSFs for the ngVLA Plains+Quarter Core subarray over a range of resolutions, showing the effect of different imaging weights (TA: uv-taper in mas, R: Briggs robust parameter). The PSFs are a selection of the data presented in Table 4. These examples illustrate how combinations of robustness and tapering allow for a beam of much higher quality (but at the expense of sensitivity).

2.5 ngVLA Plains+10th Core Subarray

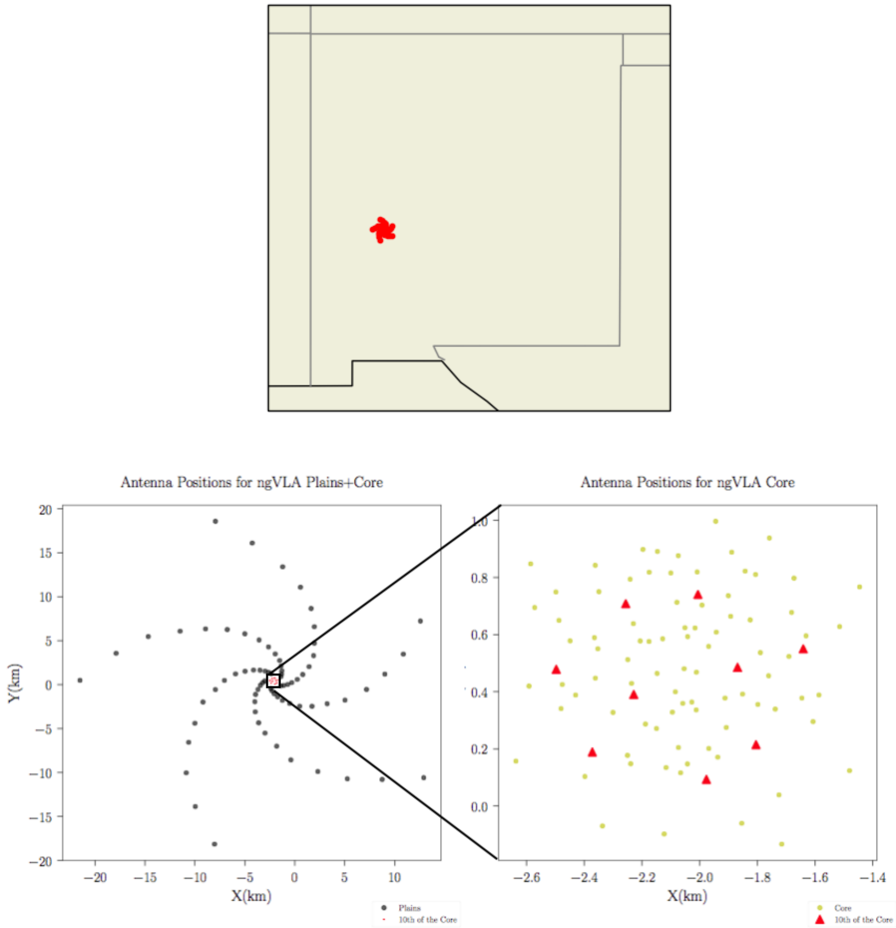

Figure 13: Positions of the 83 18 m antennas for the Plains+10th Core antennas subarray.

Figure 13 shows the position of the antennas of the (selected) Plains+10th Core subarray. The Plains+10th Core subarray extends over a maximum baseline of 36.5 km and a minimum baseline of 189 m. For this subarray, the images have a size of 20480 px.

Natural weighting with no uv-taper, which gives the best sensitivity, produces an angular resolution of 104.65 mas. From Figure 14 we see that for natural weighting, we can use a uv-taper to vary the angular resolution over a range of

$\theta_{1/2} \sim 68 - 480$ mas for which we pay a penalty in sensitivity of $\lesssim 2$. Likewise, for a range of angular resolution of $\theta_{1/2} \sim 70 - 290$ mas we pay a penalty in sensitivity of $\lesssim 1.5$.

Figure 15 shows examples of 1D East-West cuts through example PSFs.

Table 10 in Appendix B shows the key performance metrics of the ngVLA Plains+10th Core subarray using 83 antennas, tabulated for a range of selected resolutions between 100 and 10000 mas. These metrics include the change in sensitivity corresponding to the uv-taper needed to achieve these resolutions (based on Figure 14 and the frequency scaling described in Section 1).

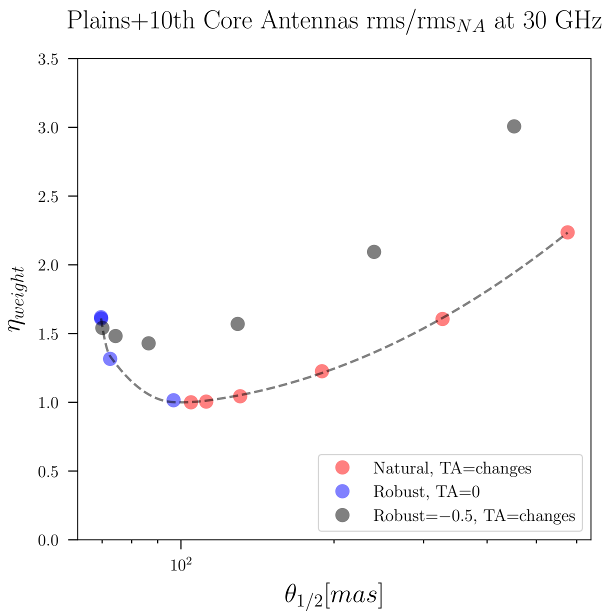

Figure 14: Taperability curve for the ngVLA Plains+10th core antennas subarray showing the image noise (rms) at different angular resolutions (FWHM) achieved by varying the imaging weights, simulated at 30 GHz. The noise has been scaled relative to that of the naturally weighted image (rms$_{NA}$). Symbols and colors are the same as used in Figure 2.

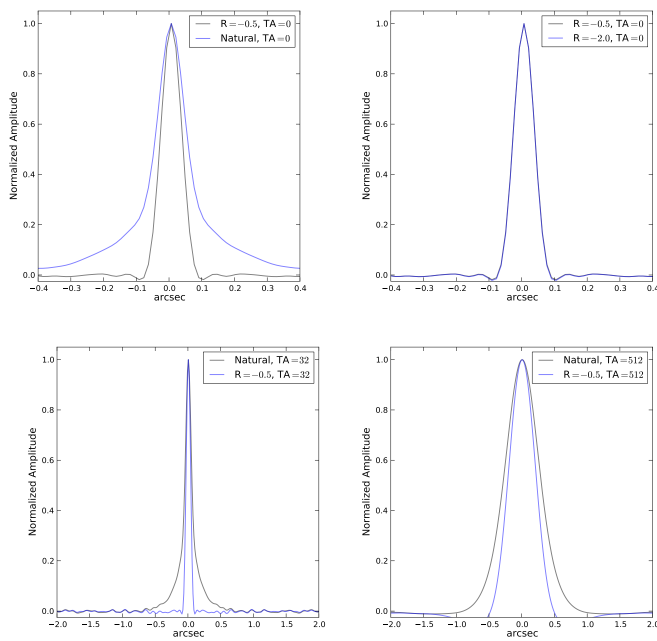

Figure 15: Simulated 30 GHz PSFs for the ngVLA Plains+10th Core subarray over a range of resolutions, showing the effect of different imaging weights (TA: uv-taper in mas, R: Briggs robust parameter). The PSFs are a selection of the data presented in Table 5. These examples illustrate how combinations of robustness and tapering allow for a beam of much higher quality (but at the expense of sensitivity).

3 Analisys

In this analysis I include the taperability results of the Plains+(Full) Core presented in ngVLA memo #55 [3], thus I will compare the features of six subarrays that contain the Plains plus fractions of the Core.

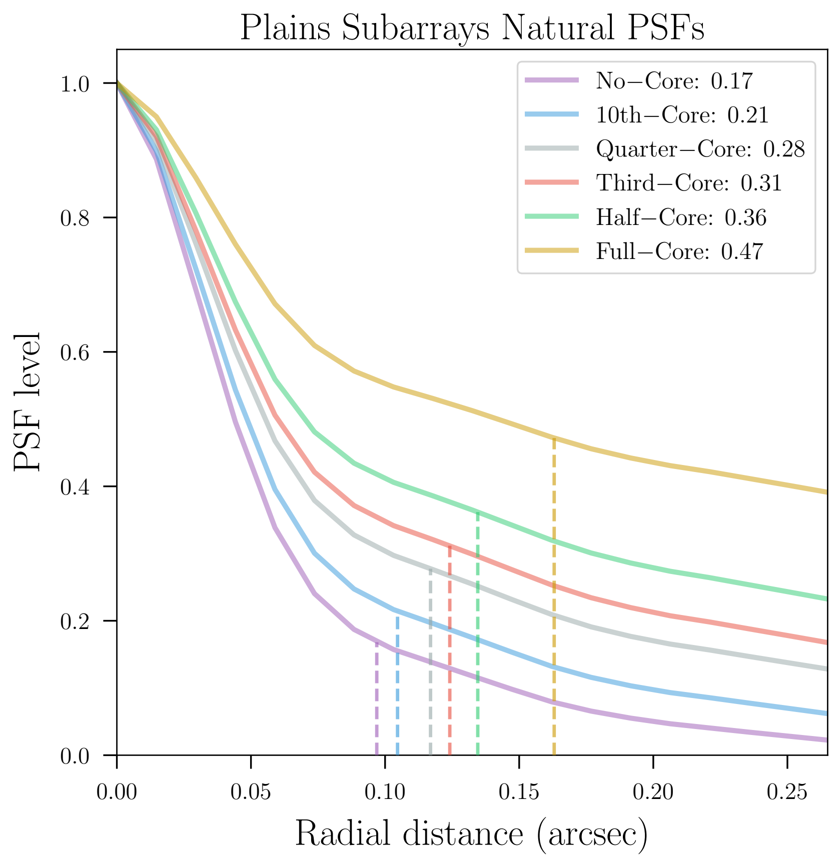

Figure 16: Radially-averaged PSF profiles of the naturally weighted synthesized beam (solid lines) for the six subarrays considered in this work. Spline interpolation is used to determine the level of the PSF at a radius of one FWHM as marked by the dashed lines.

The ngVLA memo #65 [4] introduced a set of PSF quality metrics as part of the effort to sculpt the synthesized beam in order to meet the science requirements of the KSGs. Specifically, "metric 2b" refers to a measure of the level of the PSF at a radius of one FWHM, and it is sensitive to the broad skirt seen in the naturally weighted beams for several ngVLA subarrays. Figure 16 shows radially-averaged PSF profiles[2]; spline interpolation is used to determine the level of the PSF at a radius of one FWHM (i. e., metric 2b) as marked by the dashed lines. It was suggested in ngVLA memo #47 that a skirt which raises the PSF to a level of 10% at a radius of one FWHM may be acceptably low (for comparison, a Gaussian beam is ∼6% at a radius of one FWHM). At this radius, the naturally weighted beams for our selected subarrays are far above 10% as we can see in Figure 16. This is the case even for the Plains alone subarray where there is no contribution from the Core and the PSF level at one FWHM is of about 17%, thus indicating that this configuration is still substantially centrally condensed and contains a considerable amount of short baselines.

Figure 17 shows a compilation of all the taperability curves for the six subarrays studied in this memo and (five of them) presented in Section 2: the figure in the left shows the curves that are derived from the red (uv-taper and natural weights) and the blue (Briggs robust weighting without a taper) symbols in the taperability figures and the figure to the right shows the curves corresponding to the gray symbols (Briggs robust R= −0.5 and a varying uv-taper). From the left figure we can see that the Plains plus fractions of the Core allow a range of resolutions of $68 \lesssim \theta(\mathrm{mas}) \lesssim 2700$ (and for $\eta_{weight} < 2$), with the Plains+Full−Core offering the widest range of resolutions.

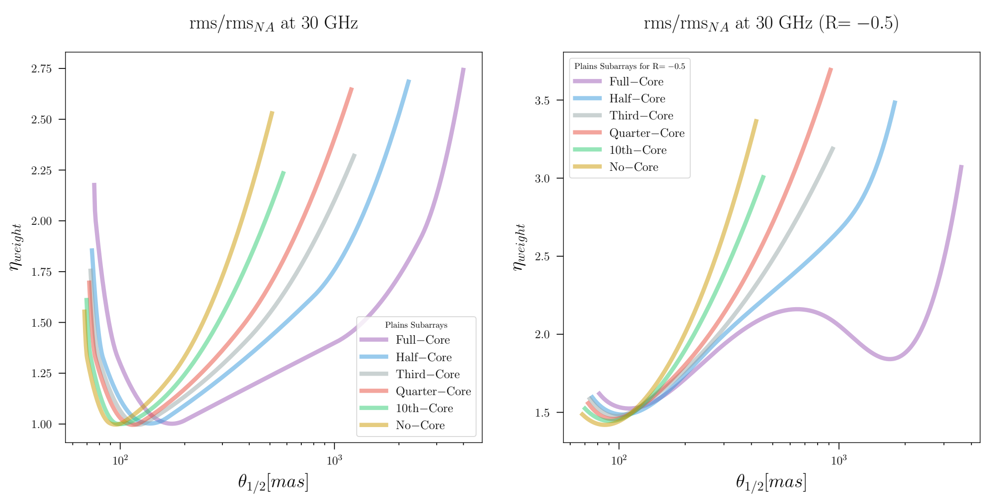

Figure 17: Compilation of taperability curves for the six subarrays studied in this memo and presented in Section 2: (left) curves composed by the red (uv-taper and natural weights) and blue (Briggs robust weighting without a taper) symbols; (right) curves composed by the gray symbols (Briggs robust R= −0.5 and a varying uv-taper).

[2] Radially-averaged profiles are produced using the 3rd party CASA task `iring`, obtained from the ALMA Nordic Node.

Figure 18 shows the same curves as in Figure 17 but now they have been re-scaled to take into account the different number of antennas per subarray by dividing each curve by the maximum sensitivity of the Plains+Full−Core (σ_{P+C})[3]. From 18 we can directly compare the sensitivities of our selected subarrays, for instance at a resolution of 200 mas the Plains+Full−Core subarray is about 1.5 times more sensitive than the Plains+Half of the Core subarray, and thus it will take the latter around 2.2 times longer to achieve a similar sensitivity than with the full Core. Alternatively, for a resolution of 1 arcsec the Plains+Full−Core subarray is about 1.7 times more sensitive than the Plains+Half of the Core subarray, and thus it will take the latter around 3 times longer time to achieved a similar sensitivity than with the full Core.

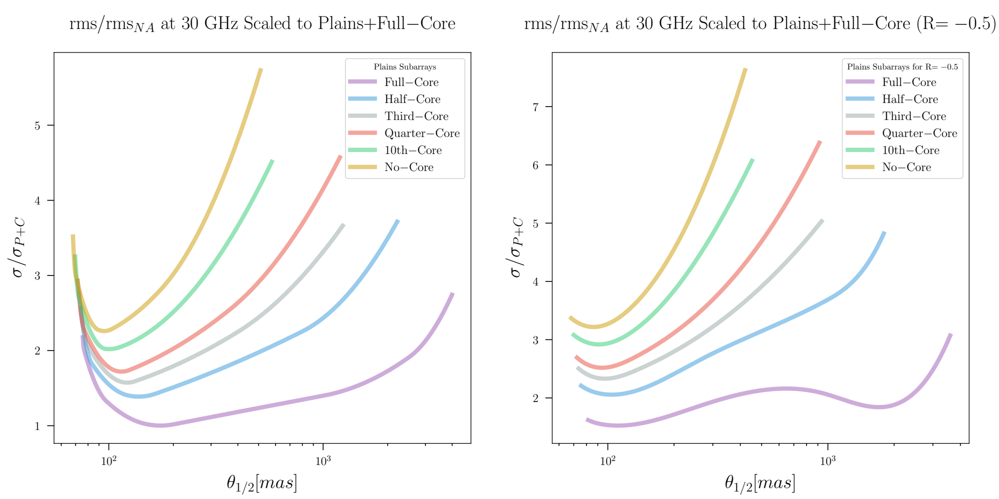

Figure 18: Curves are the same as in Figure 17 but now they have been re-scaled to take into account the different number of antennas per subarray by dividing each curve by the highest sensitivity of the Plains+Full−Core (σ_{P+C})

An alternative way to summarize the taperability curves is to plot slices at constant resolutions. Figures 19 and 20 show the values of each taperability curve at selected resolution values between 75 mas and 1 arcsec for the two different weighting schemes described previously. This abscissa is labeled according to the number of core antennas in the subarray (bottom axis) and the corresponding name given to the subarray (top axis); linear interpolation is used between each simulated subarray.

Figure 19 makes it clear that different subarrays are more efficient at different resolutions. Subarrays with fewer antennas in the core have higher native resolutions and therefore suffer less of a sensitivity penalty when using image weights

[3]For the 4−hour simulations $\sigma_{P+C} = 50\,\mu$Jy/beam.

to achieve a higher resolution PSF. On the other hand, subarrays with more core antennas can be tapered to lower resolutions with less of a sensitivity penalty. It is important to note that regardless of the inefficiency factor, the Plains + Full Core subarray will always yield the highest sensitivity of any of the Plains + Core subarrays studied here, at all resolutions, because it has the most antennas.

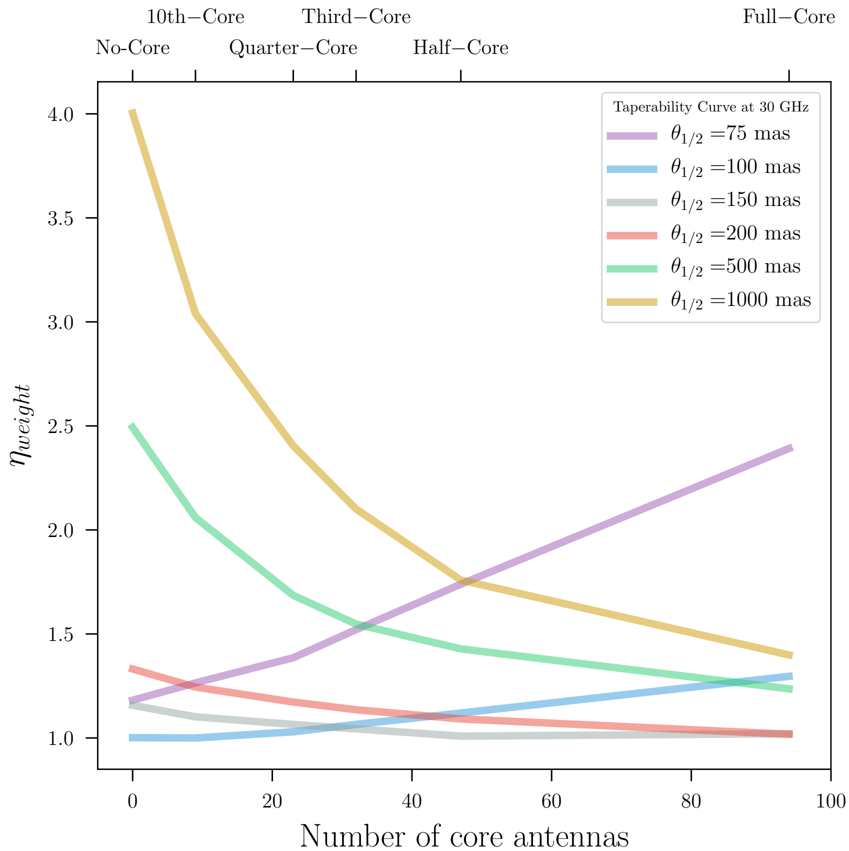

Figure 19: Efficiency curves for different selected resolutions and subarrays for uv-taper and natural weights and Briggs robust weighting without a taper (red and blue data series in the taperability figures).

Another important factor to consider when comparing these subarrays is the loss of sensitivity due to reducing the skirt of the PSF. Figure 21 summarizes the height of the skirt using metric 2b (see Figure 16) for all simulated subarrays and for both uv-taper and natural weights plus Briggs robust weighting without a taper (red solid line) and robust R= −0.5 weighting (gray solid line). For the

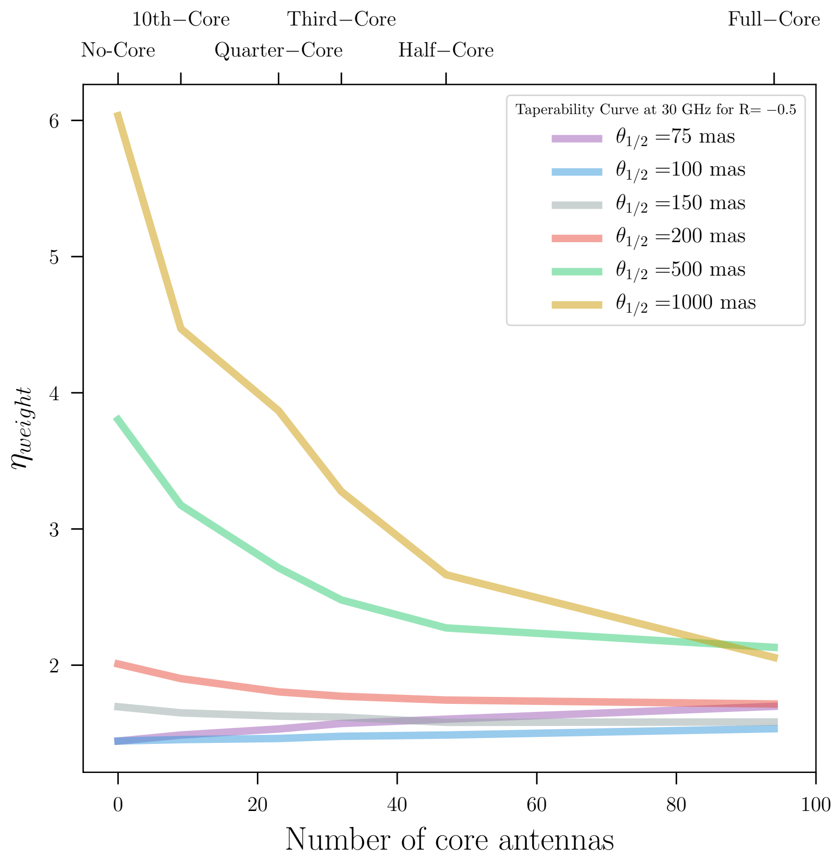

Figure 20: Efficiency curves for different selected resolutions and subarrays for Briggs robust R= −0.5 and a varying uv-taper.

former weighting scheme, the height of the skirt increases monotonically with an increasing number of core antennas. All subarrays have a skirt that exceeds the recommended level of 10% at a radius of one FWHM, even the Plains subarray alone, which has a level of ∼ 17%. This indicates that some degree of beam sculpting will be required for all of these subarrays. For the other weighting scheme studied here, robust −0.5, all subarrays have a skirt that is well below 10%.

It would be interesting to determine the precise value of robust weighting and the corresponding penalty in sensitivity needed to produce a skirt at the 10% level for each of these subarrays. Presumably, the subarrays for which the naturally-weighted skirt is lower would require less severe imaging weights (robust values closer to natural) and therefore suffer less of a sensitivity penalty. Demonstrating this quantitatively would involve the creation of many more simulated images and is currently not within the scope of this memo.

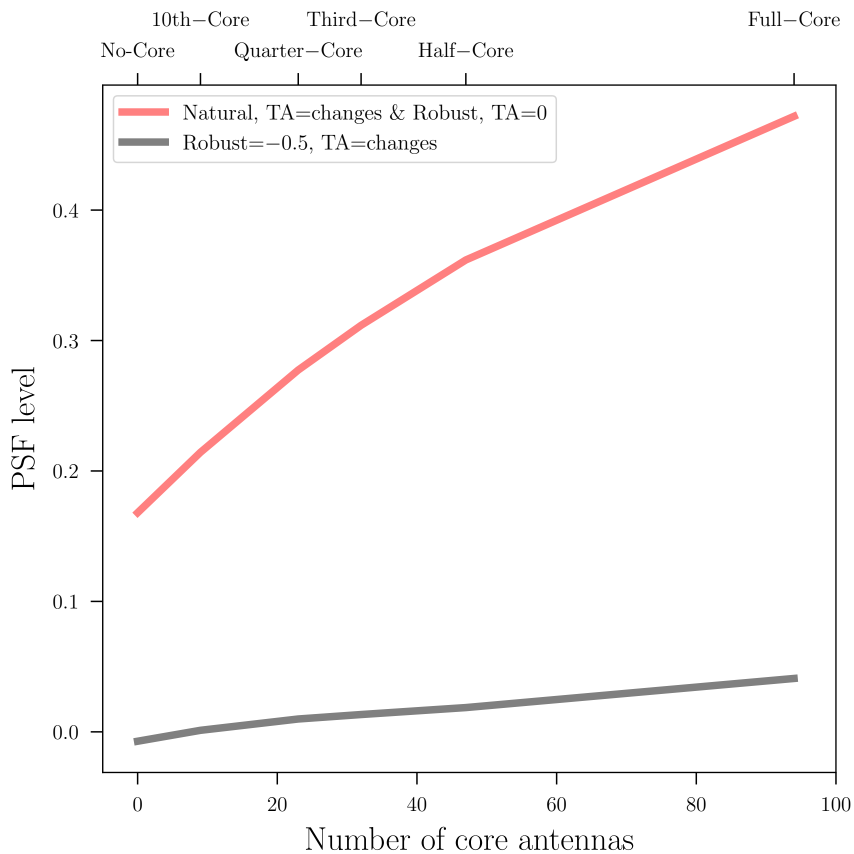

Figure 21: PSF level or height of the skirt using metric 2b (see Figure 16) for all simulated subarrays and for both uv-taper and natural weights plus Briggs robust weighting without a taper (red solid line) and robust R= -0.5 weighting and changing uv taper (gray solid line).

4 Conclusions

We have studied six subarrays including the Plains, Plains+Core, and intermediate subarrays containing the Plains plus different fractions of the Core. The Plains+Core subarray has the highest performance (as measured by sensitivity) because it has the largest number of antennas out of all the subarrays considered, but it does not always use these antennas efficiently. Specifically, the large number of core antennas in this subarray produce a large PSF skirt that must be reduced by decreasing the weight of the core antennas. The Plains+Core subarray also requires more extreme imaging weights to achieve resolutions near its diffraction limit, further reducing its efficiency.

We have shown that instead of reducing the weight of all core antennas, we can construct alternate subarrays having fewer core antennas, and that these subarrays are more efficient at certain resolutions than the full Plains+Core. A subarray's efficiency becomes important when considering the throughput of the entire ngVLA, provided that the other antennas can also be grouped into efficient subarrays and used simultaneously for other projects.

Appendix A Tables of the Simulation Parameters and Statistics

Table 1: Plains Simulation Parameters and Statistics.

Robust	Taper [mas]	Cell [mas]	Beam [mas]×[mas]	rms/rms$_{NA}$	σ/σ_{NA}
−2.0	0.0	14	71.184 × 65.063	1.561e+00	1.561e+00
−1.0	0.0	14	71.219 × 65.090	1.554e+00	1.554e+00
+0.0	0.0	14	73.417 × 66.789	1.306e+00	1.306e+00
+1.0	0.0	14	92.926 × 86.664	1.013e+00	1.013e+00
Natural	0.0	14	100.264 × 93.663	1.000e+00	1.000e+00
Natural	32.0	14	105.913 × 100.957	1.005e+00	1.005e+00
Natural	64.0	14	123.512 × 118.457	1.049e+00	1.049e+00
Natural	128.0	14	175.681 × 173.168	1.254e+00	1.254e+00
Natural	256.0	14	296.997 × 294.755	1.704e+00	1.704e+00
Natural	512.0	14	511.075 × 509.431	2.531e+00	2.531e+00
−0.5	0.0	14	71.642 × 64.846	1.503e+00	1.503e+00
−0.5	32.0	14	75.645 × 69.293	1.447e+00	1.447e+00

Table 1 – Continued on next page

Table 1 – Continued from previous page

Robust	Taper [mas]	Cell [mas]	Beam [mas]×[mas]	rms/rms$_{NA}$	σ/σ_{NA}
−0.5	64.0	14	87.273 × 81.513	1.402e+00	1.402e+00
−0.5	128.0	14	127.903 × 123.112	1.572e+00	1.572e+00
−0.5	256.0	14	232.562 × 226.191	2.192e+00	2.192e+00
−0.5	512.0	14	424.123 × 416.226	3.366e+00	3.366e+00

Table 2: Plains+Half Core Parameters and Statistics.

Robust	Taper [mas]	Cell [mas]	Beam [mas]×[mas]	rms/rms$_{NA}$	σ/σ_{NA}
−2.0	0.0	14	77.376 × 70.379	1.869e+00	1.869e+00
−1.0	0.0	14	77.623 × 70.581	1.821e+00	1.821e+00
+0.0	0.0	14	86.669 × 79.699	1.318e+00	1.318e+00
+1.0	0.0	14	126.780 × 121.001	1.021e+00	1.021e+00
Natural	0.0	14	137.492 × 131.689	1.000e+00	1.000e+00
Natural	32.0	14	145.478 × 139.917	1.003e+00	1.003e+00
Natural	64.0	14	167.846 × 162.992	1.031e+00	1.031e+00
Natural	128.0	14	245.410 × 242.307	1.154e+00	1.154e+00
Natural	256.0	14	439.342 × 435.500	1.369e+00	1.369e+00
Natural	512.0	14	799.880 × 798.148	1.646e+00	1.646e+00
Natural	1024.0	14	1376.763 × 1357.084	2.022e+00	2.022e+00
Natural	2048.0	14	2238.724 × 2193.899	2.689e+00	2.689e+00
−0.5	0.0	14	79.328 × 72.079	1.611e+00	1.611e+00
−0.5	32.0	14	83.637 × 76.284	1.551e+00	1.551e+00
−0.5	64.0	14	95.164 × 88.636	1.481e+00	1.481e+00
−0.5	128.0	14	139.774 × 134.933	1.559e+00	1.559e+00
−0.5	256.0	14	260.457 × 253.324	1.895e+00	1.895e+00
−0.5	512.0	14	502.665 × 493.444	2.276e+00	2.276e+00
−0.5	1024.0	14	959.225 × 948.250	2.632e+00	2.632e+00
−0.5	2048.0	14	1801.983 × 1786.329	3.484e+00	3.484e+00

Table 3: Plains+Third Core Parameters and Statistics.

Robust	Taper [mas]	Cell [mas]	Beam [mas]×[mas]	rms/rms$_{NA}$	σ/σ_{NA}
−2.0	0.0	14	76.303 × 69.237	1.766e+00	1.766e+00
−1.0	0.0	14	76.399 × 69.293	1.742e+00	1.742e+00
+0.0	0.0	14	82.619 × 75.046	1.324e+00	1.324e+00
+1.0	0.0	14	116.324 × 110.603	1.020e+00	1.020e+00
Natural	0.0	14	126.957 × 121.369	1.000e+00	1.000e+00
Natural	32.0	14	134.349 × 129.015	1.003e+00	1.003e+00
Natural	64.0	14	154.903 × 150.279	1.035e+00	1.035e+00
Natural	128.0	14	225.141 × 222.198	1.175e+00	1.175e+00
Natural	256.0	14	398.539 × 394.643	1.434e+00	1.434e+00
Natural	512.0	14	718.974 × 714.876	1.792e+00	1.792e+00
Natural	1024.0	14	1238.015 × 1230.062	2.323e+00	2.323e+00
−0.5	0.0	14	77.387 × 70.132	1.601e+00	1.601e+00
−0.5	32.0	14	81.761 × 74.389	1.539e+00	1.539e+00
−0.5	64.0	14	93.453 × 86.773	1.471e+00	1.471e+00
−0.5	128.0	14	137.582 × 132.561	1.563e+00	1.563e+00
−0.5	256.0	14	257.216 × 250.143	1.941e+00	1.941e+00
−0.5	512.0	14	497.811 × 488.184	2.451e+00	2.451e+00
−0.5	1024.0	14	945.926 × 926.359	3.192e+00	3.192e+00

Table 4: Plains+Quarter Core Parameters and Statistics.

Robust	Taper [mas]	Cell [mas]	Beam [mas]×[mas]	rms/rms$_{NA}$	σ/σ_{NA}
−2.0	0.0	14	75.196 × 68.299	1.704e+00	1.704e+00
−1.0	0.0	14	75.292 × 68.377	1.686e+00	1.686e+00
+0.0	0.0	14	80.416 × 72.925	1.311e+00	1.311e+00
+1.0	0.0	14	111.045 × 103.708	1.017e+00	1.017e+00
Natural	0.0	14	120.583 × 113.432	1.000e+00	1.000e+00
Natural	32.0	14	127.285 × 122.042	1.004e+00	1.004e+00

Table 4 – Continued on next page

Table 4 – Continued from previous page

Robust	Taper [mas]	Cell [mas]	Beam [mas]×[mas]	rms/rms$_{NA}$	σ/σ_{NA}
Natural	64.0	14	146.707 × 142.189	1.038e+00	1.038e+00
Natural	128.0	14	212.329 × 209.543	1.194e+00	1.194e+00
Natural	256.0	14	372.891 × 369.982	1.495e+00	1.495e+00
Natural	TA512.0	14	673.166 × 670.207	1.940e+00	1.940e+00
Natural	1024.0	14	1219.309 × 1175.590	2.649e+00	2.649e+00
−0.5	0.0	14	76.043 × 69.001	1.572e+00	1.572e+00
−0.5	32.0	14	80.426 × 73.258	1.512e+00	1.512e+00
−0.5	64.0	14	92.188 × 85.692	1.449e+00	1.449e+00
−0.5	128.0	14	135.750 × 130.869	1.558e+00	1.558e+00
−0.5	256.0	14	253.158 × 245.855	1.991e+00	1.991e+00
−0.5	512.0	14	485.706 × 475.574	2.648e+00	2.648e+00
−0.5	1024.0	14	917.550 × 912.197	3.697e+00	3.697e+00

Table 5: Plains+10th Core Parameters and Statistics.

Robust	Taper [mas]	Cell [mas]	Beam [mas]×[mas]	rms/rms$_{NA}$	σ/σ_{NA}
−2.0	0.0	14	72.942 × 66.486	1.619e+00	1.619e+00
−1.0	0.0	14	72.991 × 66.526	1.609e+00	1.609e+00
+0.0	0.0	14	76.122 × 69.188	1.316e+00	1.316e+00
+1.0	0.0	14	99.991 × 93.553	1.015e+00	1.015e+00
Natural	0.0	14	107.388 × 101.974	1.000e+00	1.000e+00
Natural	32.0	14	114.679 × 109.628	1.005e+00	1.005e+00
Natural	64.0	14	132.912 × 128.643	1.044e+00	1.044e+00
Natural	128.0	14	190.700 × 188.064	1.226e+00	1.226e+00
Natural	256.0	14	328.253 × 325.573	1.606e+00	1.606e+00
Natural	512.0	14	576.897 × 575.087	2.236e+00	2.236e+00
−0.5	0.0	14	73.404 × 66.865	1.541e+00	1.541e+00
−0.5	32.0	14	77.679 × 71.216	1.482e+00	1.482e+00
−0.5	64.0	14	89.516 × 83.380	1.429e+00	1.429e+00

Table 5 – Continued on next page

Table 5 – Continued from previous page

Robust	Taper [mas]	Cell [mas]	Beam [mas]×[mas]	rms/rms$_{NA}$	σ/σ_{NA}
−0.5	128.0	14	131.520 × 127.117	1.570e+00	1.570e+00
−0.5	256.0	14	242.855 × 236.727	2.094e+00	2.094e+00
−0.5	512.0	14	456.642 × 447.575	3.007e+00	3.007e+00

Appendix B Key Performance Metrics

Table 6: Next Generation VLA Plains Subarray Key Perform Metrics

Parameters [units]	2.4 GHz	8 GHz	16 GHz	27 GHz	41 GHz	93 GHz	Notes
Band Lower Frequency, f_L [GHz]	1.2	3.5	12.3	20.5	30.5	70.0	a
Band Upper Frequency, f_U [GHz]	3.5	12.3	20.5	34.0	50.5	116.0	a
Field of view [arcmin]	24.3	7.3	3.6	2.2	1.4	0.6	b
Aperture efficiency [%]	0.77	0.76	0.87	0.85	0.81	0.58	b
Total effective area, A_{eff} [10^3 m^2]	14.5	14.3	16.3	15.9	15.3	10.9	b
System temperature, T_{sys} [K]	25	27	28	35	56	103	a,f
Max. inst. bandwidth [GHz]	2.3	8.8	8.2	13.5	20.0	20.0	a
Antenna SEFD [Jy]	372.3	419.1	372.1	485.1	809.0	2080.5	a, b
Resolution of max. baseline (θ_{max}) [mas]	715.70	214.71	107.36	63.62	41.90	18.47	c
Natural Resolution							
Continuum rms, 1 hr [μJy/beam]	1.27	0.73	0.67	0.68	0.94	2.41	d
Line width, 10 km/s [kHz]	80.1	266.9	533.7	900.6	1367.6	3102.1	
Line rms, 1 hr, 10 km/s [μJy/beam]	215.3	132.8	83.3	83.6	113.2	193.3	d

Table 6 – Continued on next page

Table 6 – Continued from previous page

10000 mas Resolution ($\theta_{1/2}$)							
Continuum rms, 1 hr, Robust [μJy/beam]	4.39	5.17	6.66	8.47	13.68	47.01	e
Line rms, 1 hr, 10 km/s, Robust [μJy/beam]	744.4	939.0	825.0	1036.7	1653.8	3774.3	e
TB rms continuum, 1 hr, Robust [K]	0.00927	0.00098	0.00032	0.00014	0.00010	0.00007	e
TB rms line, 1 hr, 10 km/s, Robust [K]	1.5716	0.1784	0.0392	0.0173	0.0120	0.0053	e
1000 mas Resolution ($\theta_{1/2}$)							
Continuum rms, 1 hr, Robust [μJy/beam]	1.38	1.16	1.75	2.55	4.55	18.39	e
Line rms, 1 hr, 10 km/s, Robust [μJy/beam]	233.53	211.54	217.53	312.71	550.46	1476.83	e
TB rms continuum, 1 hr, Robust [K]	0.2909	0.0221	0.0083	0.0043	0.0033	0.0026	e
TB rms line, 1 hr, 10 km/s, Robust [K]	49.30	4.02	1.03	0.52	0.40	0.21	e
100 mas Resolution ($\theta_{1/2}$)							
Continuum rms, 1 hr, Robust [μJy/beam]	–	–	–	0.68	1.04	4.26	e
Line rms, 1 hr, 10 km/s, Robust [μJy/beam]	–	–	–	83.85	125.94	341.73	e
TB rms continuum, 1 hr, Robust [K]	–	–	–	0.11	0.08	0.06	e
TB rms line, 1 hr, 10 km/s, Robust [K]	–	–	–	13.99	9.11	4.80	e

Table 6 – Continued on next page

Table 6 – Continued from previous page

a – 6-band 'baseline' receiver configuration.
b – Reference design concept of 74 18m aperture antennas. Unblocked aperture with 160 μm surface.
c – Current reference design configuration. Resolution in EW axis.
d – Point source sensitivity using natural imaging weights, dual polarization.
e – Using Weights as described in the text, scaled by frequency.
f – Average over band. Assumes 1 mm PWV at 93 GHz, 6 mm PWV for other bands, 45 deg elevation on sky.
For the latest performance estimates please visit the ngVLA website: **ngvla.nrao.edu/page/refdesign**

Table 7: Next Generation VLA Plains+Half Core Subarray Key Perform Metrics

Parameters [units]	2.4 GHz	8 GHz	16 GHz	27 GHz	41 GHz	93 GHz	Notes
Band Lower Frequency, f_L [GHz]	1.2	3.5	12.3	20.5	30.5	70.0	a
Band Upper Frequency, f_U [GHz]	3.5	12.3	20.5	34.0	50.5	116.0	a
Field of view [arcmin]	24.3	7.3	3.6	2.2	1.4	0.6	b
Aperture efficiency [%]	0.77	0.76	0.87	0.85	0.81	0.58	b
Total effective area, A_{eff} [10^3 m^2]	23.7	23.3	26.7	26.1	25.0	17.8	b
System temperature, T_{sys} [K]	25	27	28	35	56	103	a,f
Max. inst. bandwidth [GHz]	2.3	8.8	8.2	13.5	20.0	20.0	a
Antenna SEFD [Jy]	372.3	419.1	372.1	485.1	809.0	2080.5	a, b
Resolution of max. baseline (θ_{max}) [mas]	715.70	214.71	107.36	63.62	41.90	18.47	c
Natural Resolution							
Continuum rms, 1 hr [μJy/beam]	0.77	0.45	0.41	0.42	0.57	1.47	d
Line width, 10 km/s [kHz]	80.1	266.9	533.7	900.6	1367.6	3102.1	
Line rms, 1 hr, 10 km/s [μJy/beam]	131.3	81.0	50.8	51.0	69.0	117.9	d

Table 7 – Continued on next page

Table 7 – Continued from previous page

10000 mas Resolution ($\theta_{1/2}$)							
Continuum rms, 1 hr, Robust [μJy/beam]	1.26	1.34	1.87	2.53	4.30	16.09	e
Line rms, 1 hr, 10 km/s, Robust [μJy/beam]	214.0	243.3	231.3	310.3	520.1	1291.6	e
TB rms continuum, 1 hr, Robust [K]	0.00267	0.00025	0.00009	0.00004	0.00003	0.00002	e
TB rms line, 1 hr, 10 km/s, Robust [K]	0.4518	0.0462	0.0110	0.0052	0.0038	0.0018	e
1000 mas Resolution ($\theta_{1/2}$)							
Continuum rms, 1 hr, Robust [μJy/beam]	1.10	0.53	0.60	0.70	1.16	4.84	e
Line rms, 1 hr, 10 km/s, Robust [μJy/beam]	185.81	96.28	73.94	86.25	140.56	388.28	e
TB rms continuum, 1 hr, Robust [K]	0.2314	0.0101	0.0028	0.0012	0.0008	0.0007	e
TB rms line, 1 hr, 10 km/s, Robust [K]	39.23	1.83	0.35	0.14	0.10	0.05	e
100 mas Resolution ($\theta_{1/2}$)							
Continuum rms, 1 hr, Robust [μJy/beam]	–	–	–	0.51	0.57	1.83	e
Line rms, 1 hr, 10 km/s, Robust [μJy/beam]	–	–	–	62.43	69.22	146.55	e
TB rms continuum, 1 hr, Robust [K]	–	–	–	0.09	0.04	0.03	e
TB rms line, 1 hr, 10 km/s, Robust [K]	–	–	–	10.41	5.01	2.06	e

Table 7 – Continued on next page

Table 7 – Continued from previous page

a – 6-band 'baseline' receiver configuration. b – Reference design concept of 121 18m aperture antennas. Unblocked aperture with 160 μm surface. c – Current reference design configuration. Resolution in EW axis. d – Point source sensitivity using natural imaging weights, dual polarization. e – Using Weights as described in the text, scaled by frequency. f – Average over band. Assumes 1 mm PWV at 93 GHz, 6 mm PWV for other bands, 45 deg elevation on sky. *For the latest performance estimates please visit the ngVLA website:* **ngvla.nrao.edu/page/refdesign**

Table 8: Next Generation VLA Plains+Third Core Subarray Key Perform Metrics

Parameters [units]	2.4 GHz	8 GHz	16 GHz	27 GHz	41 GHz	93 GHz	Notes
Band Lower Frequency, f_L [GHz]	1.2	3.5	12.3	20.5	30.5	70.0	a
Band Upper Frequency, f_U [GHz]	3.5	12.3	20.5	34.0	50.5	116.0	a
Field of view [arcmin]	24.3	7.3	3.6	2.2	1.4	0.6	b
Aperture efficiency [%]	0.77	0.76	0.87	0.85	0.81	0.58	b
Total effective area, A_{eff} [10^3 m^2]	20.8	20.4	23.4	22.8	21.9	15.6	b
System temperature, T_{sys} [K]	25	27	28	35	56	103	a,f
Max. inst. bandwidth [GHz]	2.3	8.8	8.2	13.5	20.0	20.0	a
Antenna SEFD [Jy]	372.3	419.1	372.1	485.1	809.0	2080.5	a, b
Resolution of max. baseline (θ_{max}) [mas]	715.70	214.71	107.36	63.62	41.90	18.47	c
Natural Resolution							
Continuum rms, 1 hr [μJy/beam]	0.88	0.51	0.47	0.48	0.65	1.68	d
Line width, 10 km/s [kHz]	80.1	266.9	533.7	900.6	1367.6	3102.1	
Line rms, 1 hr, 10 km/s [μJy/beam]	150.0	92.5	58.0	58.3	78.9	134.7	d

Table 8 – Continued on next page

Table 8 – Continued from previous page

10000 mas Resolution ($\theta_{1/2}$)							
Continuum rms, 1 hr, Robust [μJy/beam]	1.68	1.70	2.11	2.66	4.27	14.59	e
Line rms, 1 hr, 10 km/s, Robust [μJy/beam]	284.1	308.0	262.1	325.3	515.9	1171.3	e
TB rms continuum, 1 hr, Robust [K]	0.00354	0.00032	0.00010	0.00004	0.00003	0.00002	e
TB rms line, 1 hr, 10 km/s, Robust [K]	0.5997	0.0585	0.0125	0.0054	0.0037	0.0016	e
1000 mas Resolution ($\theta_{1/2}$)							
Continuum rms, 1 hr, Robust [μJy/beam]	1.16	0.63	0.74	0.95	1.59	5.98	e
Line rms, 1 hr, 10 km/s, Robust [μJy/beam]	196.74	115.07	92.18	116.51	192.06	480.10	e
TB rms continuum, 1 hr, Robust [K]	0.2450	0.0120	0.0035	0.0016	0.0011	0.0008	e
TB rms line, 1 hr, 10 km/s, Robust [K]	41.53	2.19	0.44	0.19	0.14	0.07	e
100 mas Resolution ($\theta_{1/2}$)							
Continuum rms, 1 hr, Robust [μJy/beam]	–	–	–	0.55	0.66	2.19	e
Line rms, 1 hr, 10 km/s, Robust [μJy/beam]	–	–	–	67.54	80.22	176.06	e
TB rms continuum, 1 hr, Robust [K]	–	–	–	0.09	0.05	0.03	e
TB rms line, 1 hr, 10 km/s, Robust [K]	–	–	–	11.27	5.80	2.48	e

Table 8 – Continued on next page

Table 8 – Continued from previous page

a – 6-band 'baseline' receiver configuration. b – Reference design concept of 106 18m aperture antennas. Unblocked aperture with 160 μm surface. c – Current reference design configuration. Resolution in EW axis. d – Point source sensitivity using natural imaging weights, dual polarization. e – Using Weights as described in the text, scaled by frequency. f – Average over band. Assumes 1 mm PWV at 93 GHz, 6 mm PWV for other bands, 45 deg elevation on sky. *For the latest performance estimates please visit the ngVLA website:* **ngvla.nrao.edu/page/refdesign**

Table 9: Next Generation VLA Plains+Quarter Core Subarray Key Perform Metrics

Parameters [units]	2.4 GHz	8 GHz	16 GHz	27 GHz	41 GHz	93 GHz	Notes
Band Lower Frequency, f_L [GHz]	1.2	3.5	12.3	20.5	30.5	70.0	a
Band Upper Frequency, f_U [GHz]	3.5	12.3	20.5	34.0	50.5	116.0	a
Field of view [arcmin]	24.3	7.3	3.6	2.2	1.4	0.6	b
Aperture efficiency [%]	0.77	0.76	0.87	0.85	0.81	0.58	b
Total effective area, A_{eff} [10^3 m^2]	19.0	18.7	21.4	20.9	20.0	14.3	b
System temperature, T_{sys} [K]	25	27	28	35	56	103	a,f
Max. inst. bandwidth [GHz]	2.3	8.8	8.2	13.5	20.0	20.0	a
Antenna SEFD [Jy]	372.3	419.1	372.1	485.1	809.0	2080.5	a, b
Resolution of max. baseline (θ_{max}) [mas]	715.70	214.71	107.36	63.62	41.90	18.47	c
Natural Resolution							
Continuum rms, 1 hr [μJy/beam]	0.97	0.56	0.51	0.52	0.71	1.83	d
Line width, 10 km/s [kHz]	80.1	266.9	533.7	900.6	1367.6	3102.1	
Line rms, 1 hr, 10 km/s [μJy/beam]	164.0	101.1	63.5	63.7	86.2	147.2	d

Table 9 – Continued on next page

Table 9 – Continued from previous page

10000 mas Resolution ($\theta_{1/2}$)							
Continuum rms, 1 hr, Robust [μJy/beam]	2.07	2.23	2.83	3.60	5.82	20.08	e
Line rms, 1 hr, 10 km/s, Robust [μJy/beam]	350.3	404.4	351.3	440.7	703.6	1612.6	e
TB rms continuum, 1 hr, Robust [K]	0.00436	0.00042	0.00013	0.00006	0.00004	0.00003	e
TB rms line, 1 hr, 10 km/s, Robust [K]	0.7394	0.0768	0.0167	0.0074	0.0051	0.0023	e
1000 mas Resolution ($\theta_{1/2}$)							
Continuum rms, 1 hr, Robust [μJy/beam]	1.21	0.73	0.89	1.18	2.02	7.89	e
Line rms, 1 hr, 10 km/s, Robust [μJy/beam]	205.86	131.74	110.33	144.81	244.74	633.61	e
TB rms continuum, 1 hr, Robust [K]	0.2564	0.0138	0.0042	0.0020	0.0015	0.0011	e
TB rms line, 1 hr, 10 km/s, Robust [K]	43.46	2.50	0.52	0.24	0.18	0.09	e
100 mas Resolution ($\theta_{1/2}$)							
Continuum rms, 1 hr, Robust [μJy/beam]	–	–	–	0.58	0.74	2.53	e
Line rms, 1 hr, 10 km/s, Robust [μJy/beam]	–	–	–	70.67	89.23	203.18	e
TB rms continuum, 1 hr, Robust [K]	–	–	–	0.10	0.05	0.04	e
TB rms line, 1 hr, 10 km/s, Robust [K]	–	–	–	11.79	6.46	2.86	e

Table 9 – Continued on next page

Table 9 – Continued from previous page

a – 6-band 'baseline' receiver configuration.
b – Reference design concept of 97 18m aperture antennas. Unblocked aperture with 160 μm surface.
c – Current reference design configuration. Resolution in EW axis.
d – Point source sensitivity using natural imaging weights, dual polarization.
e – Using Weights as described in the text, scaled by frequency.
f – Average over band. Assumes 1 mm PWV at 93 GHz, 6 mm PWV for other bands, 45 deg elevation on sky.
For the latest performance estimates please visit the ngVLA website:
ngvla.nrao.edu/page/refdesign

Table 10: Next Generation VLA Plains+10th Core Subarray Key Perform Metrics

Parameters [units]	2.4 GHz	8 GHz	16 GHz	27 GHz	41 GHz	93 GHz	Notes
Band Lower Frequency, f_L [GHz]	1.2	3.5	12.3	20.5	30.5	70.0	a
Band Upper Frequency, f_U [GHz]	3.5	12.3	20.5	34.0	50.5	116.0	a
Field of view [arcmin]	24.3	7.3	3.6	2.2	1.4	0.6	b
Aperture efficiency [%]	0.77	0.76	0.87	0.85	0.81	0.58	b
Total effective area, A_{eff} [10^3 m^2]	16.3	16.0	18.3	17.9	17.1	12.2	b
System temperature, T_{sys} [K]	25	27	28	35	56	103	a,f
Max. inst. bandwidth [GHz]	2.3	8.8	8.2	13.5	20.0	20.0	a
Antenna SEFD [Jy]	372.3	419.1	372.1	485.1	809.0	2080.5	a, b
Resolution of max. baseline (θ_{max}) [mas]	715.70	214.71	107.36	63.62	41.90	18.47	c
Natural Resolution							
Continuum rms, 1 hr [μJy/beam]	1.13	0.65	0.60	0.61	0.83	2.14	d
Line width, 10 km/s [kHz]	80.1	266.9	533.7	900.6	1367.6	3102.1	
Line rms, 1 hr, 10 km/s [μJy/beam]	191.8	118.3	74.2	74.5	100.8	172.2	d

Table 10 – Continued on next page

Table 10 – Continued from previous page

10000 mas Resolution ($\theta_{1/2}$)							
Continuum rms, 1 hr, Robust [μJy/beam]	3.04	3.23	4.01	5.00	7.97	26.83	e
Line rms, 1 hr, 10 km/s, Robust [μJy/beam]	515.9	586.7	497.2	612.1	963.6	2154.6	e
TB rms continuum, 1 hr, Robust [K]	0.00643	0.00061	0.00019	0.00008	0.00006	0.00004	e
TB rms line, 1 hr, 10 km/s, Robust [K]	1.0891	0.1115	0.0236	0.0102	0.0070	0.0030	e
1000 mas Resolution ($\theta_{1/2}$)							
Continuum rms, 1 hr, Robust [μJy/beam]	1.30	0.94	1.28	1.75	2.99	11.39	e
Line rms, 1 hr, 10 km/s, Robust [μJy/beam]	220.81	170.47	158.68	213.86	361.37	914.63	e
TB rms continuum, 1 hr, Robust [K]	0.2750	0.0178	0.0061	0.0029	0.0022	0.0016	e
TB rms line, 1 hr, 10 km/s, Robust [K]	46.62	3.24	0.75	0.36	0.26	0.13	e
100 mas Resolution ($\theta_{1/2}$)							
Continuum rms, 1 hr, Robust [μJy/beam]	–	–	–	0.62	0.89	3.36	e
Line rms, 1 hr, 10 km/s, Robust [μJy/beam]	–	–	–	76.43	107.58	269.65	e
TB rms continuum, 1 hr, Robust [K]	–	–	–	0.10	0.06	0.05	e
TB rms line, 1 hr, 10 km/s, Robust [K]	–	–	–	12.75	7.78	3.79	e

Table 10 – Continued on next page

Table 10 – Continued from previous page

a – 6-band 'baseline' receiver configuration.
b – Reference design concept of 83 18m aperture antennas. Unblocked aperture with 160 μm surface.
c – Current reference design configuration. Resolution in EW axis.
d – Point source sensitivity using natural imaging weights, dual polarization.
e – Using Weights as described in the text, scaled by frequency.
f – Average over band. Assumes 1 mm PWV at 93 GHz, 6 mm PWV for other bands, 45 deg elevation on sky.
For the latest performance estimates please visit the ngVLA website: **ngvla.nrao.edu/page/refdesign**

Appendix C ngVLA Plains+Mid-baseline Subarray

Figure 22 shows the position of the antennas of the Plains+Mid-baseline subarray, which extends over a maximum baseline of 1005.4 km (minimum baseline 250 m). For this subarray, the images have a size of 40000 px.
Natural weighting with no uv-taper, which gives the best sensitivity, produces an angular resolution of 6.17 mas. From Figure 23 we see that for natural weighting, we can use a uv-taper to vary the angular resolution over a range of $\theta_{1/2} \sim 2.8 - 160$ mas for which we pay a penalty in sensitivity of $\lesssim 2$. Likewise, for a range of angular resolution of $\theta_{1/2} \sim 3.2 - 70$ mas we pay a penalty in sensitivity of $\lesssim 1.5$.

The features of the resulting taperability curve are similar to the ones from the ngVLA Main subarray, likely due to their similar ratios of short versus long baselines (i.e., many more short baselines than long baselines).

Figure 24 shows examples of 1D East-West cuts through example PSFs.
Table 12 in Appendix B shows the key performance metrics of the ngVLA Plains+Mid-baseline subarray using 120 antennas, tabulated for a range of selected resolutions between 10 and 10000 mas. These metrics include the change in sensitivity corresponding to the uv-taper needed to achieve these resolutions (based on Figure 23 and the frequency scaling described in Section 1).

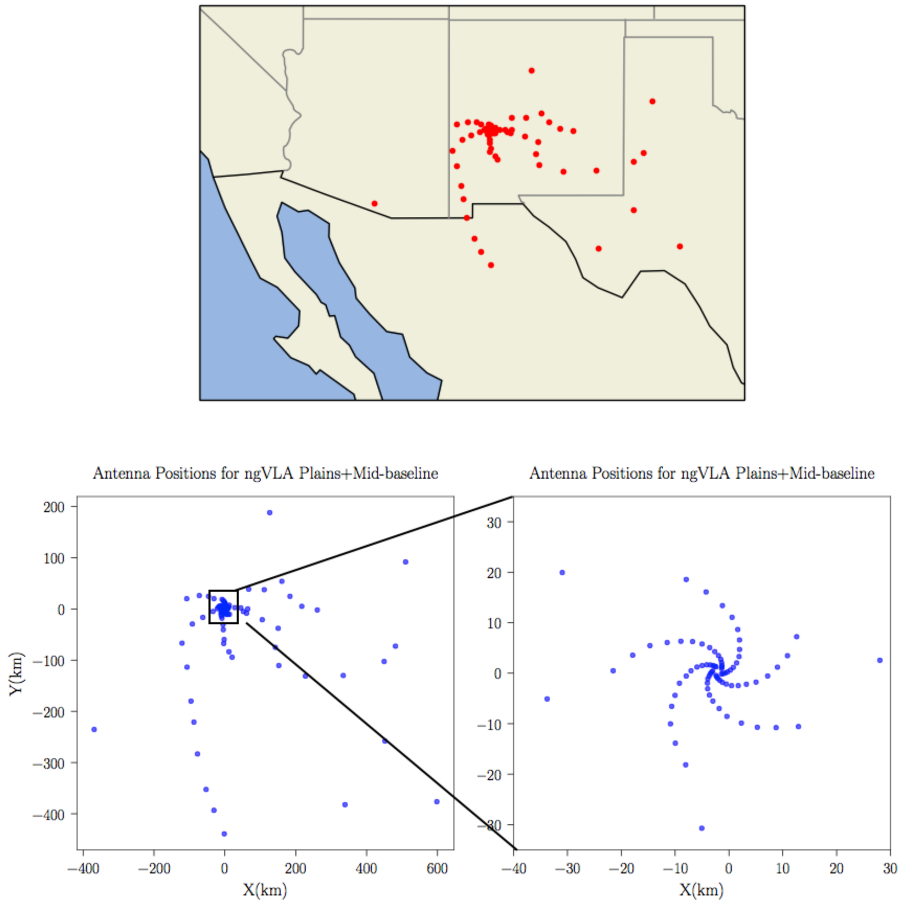

Figure 22: Positions of the 120 18 m antennas for the Plains+Mid-baseline subarray.

Table 11: Plains+Mid Simulation Parameters and Statistics.

Robust	Taper [mas]	Cell [mas]	Beam [mas]×[mas]	rms/rms$_{NA}$	σ/σ_{NA}
−2.0	0.0	0.52	3.398 × 2.283	2.041e+00	2.041e+00
−1.0	0.0	0.52	3.421 × 2.315	1.931e+00	1.931e+00
+0.0	0.0	0.52	4.218 × 3.114	1.318e+00	1.318e+00

Table 11 – Continued on next page

Table 11 – Continued from previous page

Robust	Taper [mas]	Cell [mas]	Beam [mas]×[mas]	rms/rms$_{NA}$	σ/σ_{NA}
+1.0	0.0	0.52	6.328 × 5.122	1.022e+00	1.022e+00
Natural	0.0	0.52	6.844 × 5.563	1.000e+00	1.000e+00
Natural	1.0	0.52	7.162 × 5.865	1.002e+00	1.002e+00
Natural	2.0	0.52	8.090 × 6.711	1.017e+00	1.017e+00
Natural	4.0	0.52	11.731 × 9.529	1.085e+00	1.085e+00
Natural	8.0	0.52	21.871 × 15.912	1.196e+00	1.196e+00
Natural	16.0	0.52	39.409 × 30.739	1.336e+00	1.336e+00
Natural	32.0	0.52	71.005 × 60.829	1.504e+00	1.504e+00
Natural	64.0	0.52	110.067 × 105.623	1.683e+00	1.683e+00
Natural	128.0	0.52	169.729 × 166.845	2.055e+00	2.055e+00
Natural	256.0	0.52	294.927 × 292.689	2.823e+00	2.823e+00
−0.5	0.0	0.52	3.563 × 2.494	1.623e+00	1.623e+00
−0.5	1.0	0.52	3.651 × 2.619	1.581e+00	1.581e+00
−0.5	2.0	0.52	3.963 × 3.096	1.517e+00	1.517e+00
−0.5	4.0	0.52	5.593 × 4.732	1.556e+00	1.556e+00
−0.5	8.0	0.52	10.745 × 8.047	1.760e+00	1.760e+00
−0.5	16.0	0.52	20.032 × 15.598	2.034e+00	2.034e+00
−0.5	32.0	0.52	37.683 × 31.539	2.306e+00	2.306e+00
−0.5	64.0	0.52	68.584 × 65.191	2.357e+00	2.357e+00
−0.5	128.0	0.52	117.336 × 115.905	2.427e+00	2.427e+00
−0.5	256.0	0.52	226.887 × 226.198	3.120e+00	3.120e+00

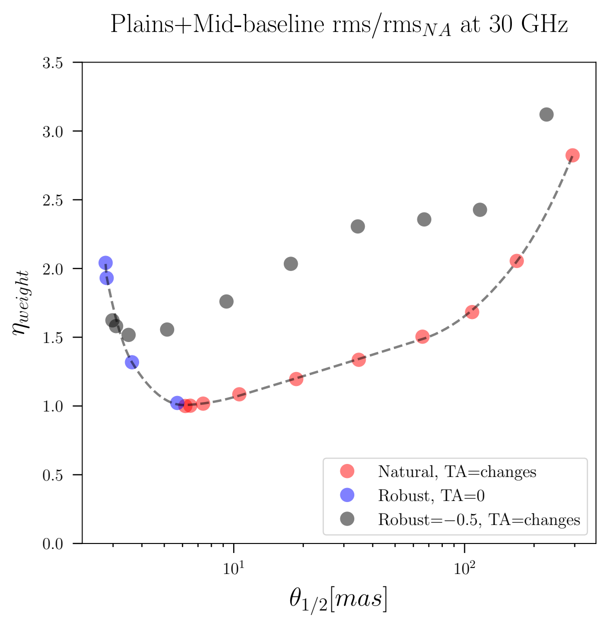

Figure 23: Taperability curve for the ngVLA Plains+Mid-baseline subarray showing the image noise (rms) at different angular resolutions (FWHM) achieved by varying the imaging weights, simulated at 30 GHz. The noise has been scaled relative to that of the naturally weighted image (rms$_{NA}$). Symbols and colors are the same as used in Figure 2.

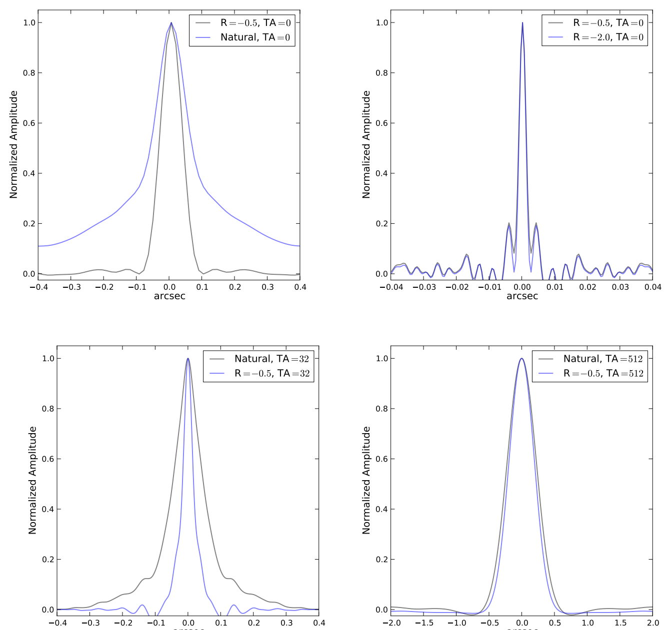

Figure 24: Simulated 30 GHz PSFs for the ngVLA Plains+Mid-baseline subarray over a range of resolutions, showing the effect of different imaging weights (TA: uv-taper in mas, R: Briggs robust parameter). The PSFs are a selection of the data presented in Table 11. These examples illustrate how combinations of robustness and tapering allow for a beam of much higher quality (but at the expense of sensitivity).

Table 12: Next Generation VLA Plains+Mid Subarray Key Perform Metrics

Parameters [units]	2.4 GHz	8 GHz	16 GHz	27 GHz	41 GHz	93 GHz	Notes
Band Lower Frequency, f_L [GHz]	1.2	3.5	12.3	20.5	30.5	70.0	a
Band Upper Frequency, f_U [GHz]	3.5	12.3	20.5	34.0	50.5	116.0	a
Field of view [arcmin]	24.3	7.3	3.6	2.2	1.4	0.6	b
Aperture efficiency [%]	0.77	0.76	0.87	0.85	0.81	0.58	b
Total effective area, A_{eff} [10^3 m^2]	23.5	23.1	26.5	25.9	24.8	17.7	b
System temperature, T_{sys} [K]	25	27	28	35	56	103	a,f
Max. inst. bandwidth [GHz]	2.3	8.8	8.2	13.5	20.0	20.0	a
Antenna SEFD [Jy]	372.3	419.1	372.1	485.1	809.0	2080.5	a, b
Resolution of max. baseline (θ_{max}) [mas]	25.64	7.69	3.85	2.28	1.50	0.66	c
Natural Resolution							
Continuum rms, 1 hr [μJy/beam]	0.78	0.45	0.41	0.42	0.58	1.48	d
Line width, 10 km/s [kHz]	80.1	266.9	533.7	900.6	1367.6	3102.1	
Line rms, 1 hr, 10 km/s [μJy/beam]	132.4	81.7	51.2	51.4	69.6	118.9	d
10000 mas Resolution ($\theta_{1/2}$)							
Continuum rms, 1 hr, Robust [μJy/beam]	4.20	4.68	5.91	7.44	11.93	40.54	e
Line rms, 1 hr, 10 km/s, Robust [μJy/beam]	711.6	850.7	733.1	911.0	1442.7	3255.2	e
TB rms continuum, 1 hr, Robust [K]	0.00886	0.00089	0.00028	0.00012	0.00009	0.00006	e
TB rms line, 1 hr, 10 km/s, Robust [K]	1.502	0.162	0.035	0.015	0.010	0.005	e

Table 12 – Continued on next page

Table 12 – Continued from previous page

1000 mas Resolution ($\theta_{1/2}$)							
Continuum rms, 1 hr, Robust [μJy/beam]	1.21	1.19	1.72	2.43	4.23	16.58	e
Line rms, 1 hr, 10 km/s, Robust [μJy/beam]	204.90	216.81	213.28	296.93	511.81	1331.64	e
TB rms continuum, 1 hr, Robust [K]	0.2552	0.0227	0.0082	0.0040	0.0031	0.0023	e
TB rms line, 1 hr, 10 km/s, Robust [K]	43.26	4.12	1.01	0.50	0.37	0.19	e
100 mas Resolution ($\theta_{1/2}$)							
Continuum rms, 1 hr, Robust [μJy/beam]	0.80	0.58	0.60	0.67	1.07	4.33	e
Line rms, 1 hr, 10 km/s, Robust [μJy/beam]	136.04	104.65	73.76	82.21	129.93	347.32	e
TB rms continuum, 1 hr, Robust [K]	16.94	1.09	0.28	0.11	0.08	0.06	e
TB rms line, 1 hr, 10 km/s, Robust [K]	2871.90	198.83	35.03	13.71	9.40	4.88	e
10 mas Resolution ($\theta_{1/2}$)							
Continuum rms, 1 hr, Robust [μJy/beam]	–	1.64	0.42	0.44	0.65	1.95	e
Line rms, 1 hr, 10 km/s, Robust [μJy/beam]	–	297.71	52.62	53.72	78.82	156.40	e
TB rms continuum, 1 hr, Robust [K]	–	311.4834	20.1637	7.3191	4.7151	2.7385	e
TB rms line, 1 hr, 10 km/s, Robust [K]	–	56564.19	2499.36	896.09	570.20	219.89	e

Table 12 – Continued on next page

Table 12 – Continued from previous page

a – 6-band 'baseline' receiver configuration.
b – Reference design concept of 120 18m aperture antennas. Unblocked aperture with 160 μm surface.
c – Current reference design configuration. Resolution in EW axis.
d – Point source sensitivity using natural imaging weights, dual polarization.
e – Using Weights as described in the text, scaled by frequency.
f – Average over band. Assumes 1 mm PWV at 93 GHz, 6 mm PWV for other bands, 45 deg elevation on sky.
For the latest performance estimates please visit the ngVLA website:
ngvla.nrao.edu/page/refdesign

Acknowledgments

Many thanks to Joan Wrobel and Brian Mason for providing important information for the development of this work. This study made use of the CASA task `iring`, an open-source tool from the Nordic ALMA regional center. The National Radio Astronomy Observatory is a facility of the National Science Foundation operated under cooperative agreement by Associated Universities, Inc.

References

[1] Chris Carilli, *Next Generation Very Large Array Memo No. 12 The Strength of the Core.*

[2] Chris Carilli, Alan Erickson, *Next Generation VLA Memo. 41 Initial Imaging Tests of the Spiral Configuration.*

[3] Viviana Rosero, *Next Generation Very Large Array Memo No. 55 Taperability Study for the ngVLA and Performance Estimates (v2).*

[4] Viviana Rosero, *Next Generation Very Large Array Memo No. 65 Sculpting of the Synthesized Beam and Image Fidelity Study of KSG 1: Imaging of Protoplanetary Disks.*

[5] Joan Wrobel, *A Notional Reference Observing Program document 020.10.15.05.10–0001–REP (v1).*